Angewandte Chemie

DOI: 10.1002/anie.200604623

Bioinorganic Chemistry

Beryllium Displacement of H^+ from Strong Hydrogen Bonds**

T. Mark McCleskey,* Deborah S. Ehler, Timothy S. Keizer, Dilip N. Asthagiri, Lawrence R. Pratt, Ryszard Michalczyk, and Brian L. Scott*

Beryllium is highly toxic both as a suspected carcinogen and as the agent that initiates chronic beryllium disease (CBD). A recent NIOSH report estimates that 26500 current US Department of Energy and Department of Defense employees as well as up to 106000 workers in the private sector have potentially been exposed to beryllium.[1] CBD, a granulomatous lung disease, is a cell-mediated immune response to inhaled beryllium in 6–20% of exposed individuals. The nature and effects of CBD have been well-studied[2] but the role of beryllium to trigger CBD and how beryllium enters the cell is not well understood.[3,4]

Most research efforts focus on biological[5] and environmental[6] effects of beryllium, and far less effort is devoted to the speciation and molecular interactions of beryllium under physiological conditions.[7–9] CBD has been correlated with a series of major histocompatibility complex (MHC) Class II antigen-presenting proteins containing a glutamic acid residue at position 69, but understanding the mechanism of CBD has proved elusive.[10] The activity and immune responses of these proteins have been studied in the presence of beryllium, but how or where beryllium binds remains unknown.[11,12] The only reported direct binding of beryllium with a protein has been with the iron-storage protein ferritin.[13] A better understanding of beryllium speciation is needed to combat the disease and address environmental concerns.

It is known that $[Be(H_2O)_4]^{2+}$ readily deprotonates and has a pK_a value of 3.8.[14] In the pH range from 4.5 to 5.5 (with 2 mM Be), a beryllium trimer $[Be_3(OH)_3(H_2O)_6]^{3+}$ is formed.[15] Above pH 5.5, beryllium precipitates as a polymeric hydroxide. Beryllium in solution is typically viewed as a dication that binds hard anions such as carboxylates, with a charge/size ratio similar to that of Al^{3+}. Herein we take a very different strategy of comparing beryllium with H^+ and show that beryllium can displace H^+ in many strong hydrogen bonds in which beryllium as a "tetrahedral proton" is thermodynamically preferred.

We chose to study beryllium binding to transferrin because of the strong hydrogen bonds observed in the crystal structure of the apo form and because it could serve as a transport vehicle to import beryllium into the cell much like it does for iron. Transferrin is highly soluble (250 μM), which allowed us to use ^{9}Be NMR spectroscopy, the only method available for direct observation of beryllium interactions and speciation in solution. Beryllium was added in solution form in an expected excess of 8 equivalents to both apo- and indium-loaded transferrin (250 μM in HEPES buffer at pH 7.1; HEPES = 2-[4-(2-hydroxyethyl)-1-piperazinyl]ethanesulfonic acid). Binding to the protein was indicated by the lack of any precipitate and confirmed by a broad peak at $\delta = 1.1$ ppm in the ^{9}Be NMR spectrum. Surprisingly, binding was observed for both the apo and the indium-loaded protein. The signal at $\delta = 1.1$ ppm for the indium-loaded proteins was less intense.

We determined the stoichiometry of binding to the apo (apoTf) and holo (holoTf) forms of transferrin by preparing a solution with excess beryllium (20 equivalents) in HEPES buffer and then purifying the solution by a combination of filtration through a 0.45-μm syringe filter to remove particulate beryllium, and concentration and washing of the filtrate with a 10000 nominal molecular weight limit (NMWL) Centriplus concentrator to remove unbound, soluble beryllium. The final beryllium concentration was determined by fluorescence analysis, and the protein concentration was verified by UV/Vis spectroscopy. A control experiment with a solution of beryllium in HEPES buffer showed no beryllium in the filtrate, which is as expected since beryllium precipitates as $Be(OH)_2$ at pH 7. The stoichiometry of binding was determined to be 12 and 7 for apoTf and holoTf, respectively. This surprisingly high number clearly shows that Be is not simply binding to the iron site in transferrin and prompted us to reevaluate the known crystal structures for potential binding sites.

The candidate beryllium binding sites in transferrin were chosen on the basis of strong hydrogen-bonding sites formed between oxygen donor residues of aspartate, glutamate, tyrosine, serine, and threonine. Previous calculations showed that beryllium prefers to bind to the oxygen sites of these residues.[16] Strong hydrogen bonds occur when the distance between the two heteroatoms, typically O−H···O or O−H···N, is shorter than the sum of the van der Waals radii and the energy barrier to hydrogen transfer between two atoms is on the order of the O−H vibrational zero-point energy. The strong hydrogen bond provides two advantages: First, it brings two oxygen atoms into a predefined chelating binding site for beryllium. The O···O distance in a strong hydrogen bond is in the range 2.4–2.8 Å, which corresponds

---

[*] T. M. McCleskey, D. S. Ehler, T. S. Keizer, D. N. Asthagiri, L. R. Pratt, R. Michalczyk, B. L. Scott
Los Alamos National Laboratory
MPA-MC
Mail Stop J514, Los Alamos, NM 87545 (USA)
Fax: (+1) 505-667-9905
E-mail: tmark@lanl.gov
bscott@lanl.gov

[**] This work was supported by the Laboratory Directed Research and Development program (LDRD) at the Los Alamos National Laboratory.

Supporting information for this article is available on the WWW under http://www.angewandte.org or from the author.

very well to the intraligand oxygen–oxygen distances of 2.26 to 2.86 Å in 383 beryllium structures in the Cambridge Structural Database.[17] Second, the strong hydrogen bond provides a low-barrier pathway to displace the proton without breaking a strong covalent O–H bond. The closer the oxygen atoms are in the hydrogen bond, the flatter the two-well potential-energy surface becomes until the crossover energy becomes lower than the zero-point energy of the O–H stretching mode.[18] Near this point, the proton can easily shift to the more acidic oxygen atom, allowing Be to interact with the basic oxygen without the energy cost of breaking a covalent O–H bond (−87.3(1.5) kcal mol^{-1}).[19] In aqueous continuum we calculated the free energy of Equation (1) to be −4.9 kcal mol^{-1}.[20]

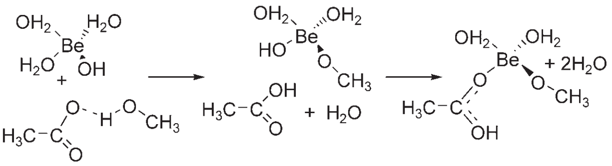

(1)

The results of using the above criteria for beryllium binding site selection from apo- and holo-transferrin proteins are shown in Table 1. For the apo form there are six relevant O···O contacts ranging from 2.47 to 3.10 Å. Five of these represent hydrogen bonds from one of the alcohol-containing amino acids threonine, serine, or tyrosine to a carboxylic acid from either aspartate or glutamate. The sixth is between two aspartate carboxylic acids. Thus there are six potential sites for apoTf and three to four for holoTf (four includes an internal site at Glu 83–Tyr 85). As the crystal structures represent only one lobe of the transferrin molecule, the whole apoTf protein has 12 potential binding sites, whereas holoTf has 6–8. These numbers agree very well with the observed numbers of 12 and 7 from the stoichiometry studies.

Table 1: Sites of strong hydrogen bonding in the crystal structures of human transferrin.[a]

Hydrogen bond	$O_{donor}\cdots O_{acceptor}$ distance [Å]	
	ApoTf	HoloTf
Glu83–Tyr85	2.53	2.62 (interior)
Ser208–Glu212	–	2.82
Tyr185–Asp197	2.69	2.77
Asp229–Thr231	2.58	2.75
Ser44–Asp47	3.02	–
Ser87–Glu89	3.10	–
Asp163–Asp166	2.47	–
total sites	6	4
accessible sites	6	3

[a] The apoTf $O_{donor}\cdots O_{acceptor}$ distances are the average values from the four crystallographically independent apoTf molecules (RCSD code 1BP5, 2.2-Å resolution). The Ser87–Glu89 distance given is the shortest value of the four apoTf molecules; the remaining three molecules have distances that are all greater than 3.66 Å. The holoTf distances are the average values from two crystal structures (RCSD codes 1A8E and 1A8F, with resolutions of 1.6 and 1.8 Å, respectively).

Quantum-chemical optimizations and ^{9}Be NMR line-shift calculations for a series of small-molecule mimics of the suspected binding sites [Gaussian 03, HF/3-21G(d)] in the gas phase[21] yielded values from $\delta = 1.6$ to 4.6 ppm. The observed value of $\delta = 1.1$ ppm for the beryllium–Tf complex agrees best with the calculated values for the mimics $[Be(H_2O)_2(MeO)(Ac)]$ ($\delta = 1.72$ ppm) and $[Be(H_2O)_2(PhO)(Ac)]$ ($\delta = 1.66$ ppm), which mimic Asp/Glu···Thr/Ser and Asp/Glu···Tyr, respectively. The broadness of the NMR peak is consistent with multiple types of binding sites in the protein. The agreement of these calculated ^{9}Be NMR line shifts with experiment values and of the predicted and measured number of binding sites strongly suggest that the beryllium dications bind at the sites outlined in Table 1 and shown in Figure 1.

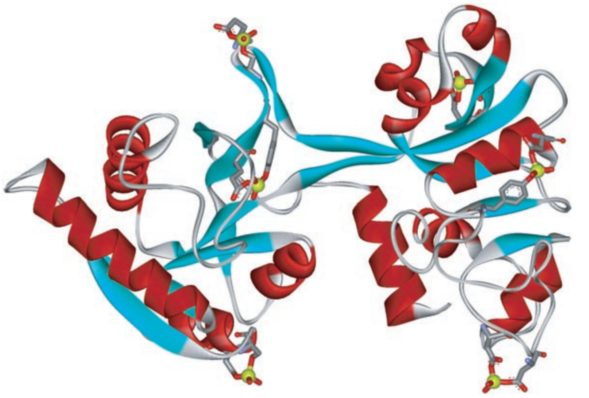

Figure 1. Predicted binding of beryllium (green) in the N lobe of apo-transferrin. The picture was produced by taking the crystal structure of the N-terminal lobe of transferrin (1BP5) and replacing the strong hydrogen bonds listed in Table 1 with $[Be(H_2O)_2]^{2+}$. The first coordination sphere of beryllium was then optimized. Additional details are given in the Supporting Information.

This type of binding through strong hydrogen bonds can be extended to explain most of the strong beryllium interactions reported in the literature. Strong hydrogen bonds can be readily identified through significant NMR chemical shifts in the range $\delta = 12$–18 ppm.[22] Table 2 shows a series of ligands that have previously been studied for beryllium binding along with their ^{1}H NMR chemical shifts and pK_a values. All of the ligands have strong hydrogen bonds, as identified by their ^{1}H NMR chemical shift, and bind

Table 2: NMR chemical shifts, log *K*, and pK_a values (of the proton in the strong hydrogen bond) for several strong Be-binding ligands.

Ligand	log *K*[7]	pK_a	δ [ppm][14]
phthalate	3.17	5.4	21
maleate	4.3	6.2	20.5
acetylacetonate	12.3	9.3	16.1
salicylate	12.4	13.7	16.3
chromotropate	16.2	15.6	17.4

beryllium well. Within the series, binding constants increase as the $\mathrm{p}K_a$ value of the proton and basicity of the site increase. The strongest ligands are chromotropic acid, salicylic acid (SA), and hydroxybenzoquinoline (HBQ). These three ligands are capable of solubilizing beryllium across an extensive pH range and compete favorably with hydrolysis reactions in solution; all have $\mathrm{p}K_a$ values greater than 13. The requirement of a strong hydrogen bond explains why beryllium is able to deprotonate and bind ligands such as HBQ and salicylate as well as the aliphatic alcohol of citric acid, yet does not exchange with the proton on a simple monodentate phenol or alcohol.

We propose that strong hydrogen bonds with high $\mathrm{p}K_a$ values make for ideal binding sites for beryllium and provide a unique kinetic pathway for beryllium binding. We have demonstrated the importance of such binding in Be protein interactions with transferrin. Transferrin binds up to 12 equivalents of Be and could serve as a vehicle for Be transport into the cell. This binding concept also has intriguing implications for the immune system, in which docking interactions to foreign carbohydrates are based on strong hydrogen bonds. For example, the crystal structure of the immune protein SP-D bound to a sugar residue shows two strong hydrogen bonds between the sugar OH groups and carboxylate residues of the protein.[24] Beryllium has the potential to replace such protons and dramatically alter binding interactions that are known to illicit immune responses.

Experimental Section

Materials: Human transferrin was purchased from Sigma. Beryllium standards in the ppb range were obtained from SPEX Certiprep. All other chemicals were purchased from Aldrich. Buffers and other solutions were prepared with Type II millipore water.

Analysis: The beryllium concentration was determined by using a modification of the Berylliant fluorescence test. The detection solution was analyzed for beryllium on a Barnstead Quantech fluorimeter. The transferrin concentration was determined by UV/Vis spectroscopy on a Hewlett Packard Model 8453 at 278 nm (extinction coefficient $93\,000\,\mathrm{M}^{-1}$).

Calculations: The individual Gibbs free energies were calculated by using Gaussian 03 at the DFT/6-31G(d) level. We calculated the energetics of the reaction with Gaussian 03.

NMR spectra: All NMR spectra were recorded on a Bruker Avance 500-MHz spectrometer with a tunable broadband probe with z gradients. The initial sample contained 0.36 mM transferrin in 0.1 M HEPES, 5 mM sodium bicarbonate buffer (pH 7.0) in $90\%\,H_2O/10\%\,D_2O$ and was titrated with 1.11 M Be^{2+} solution to achieve final Be^{2+} concentrations of 0.9, 1.8, 2.7, 3.6, 4.5, and 5.4 mM, corresponding to 2.5–15 equivalents of Be^{2+}/protein molecule.

Details for the preparation of the In-loaded transferrin and the stoichiometry experiments are given in the Supporting Information.

Received: November 13, 2006

Keywords: beryllium · bioinorganic chemistry · hydrogen bonds · metalloproteins

[1] P. K. Henneberger, S. K. Goe, W. E. Miller, B. Doney, D. W. Groce, *J. Occup. Environ. Hyg.* **2004**, *1*, 648 – 659.
[2] C. Saltini, M. Amicosante, *Am. J. Med. Sci.* **2001**, *321*, 89 – 98.
[3] M. Eisenbud, *Appl. Occup. Environ. Hyg.* **1998**, *13*, 25 – 31.
[4] C. Saltini, M. Amicosante, A. Franchi, G. Lombardi, L. Richeldi, *Eur. Respir. J.* **1998**, *12*, 1463 – 1475.
[5] M. D. Rossman, O. P. Preuss, M. B. Powers, *Beryllium: Biomedical and Environmental Aspects*, Williams and Wilkens, Baltimore, **1991**.
[6] T. P. Taylor, M. Ding, D. S. Ehler, T. M. Foreman, J. P. Kaszuba, N. N. Sauer, *J. Environ. Sci. Health Part A* **2003**, *38*, 439 – 469.
[7] L. Alderighi, P. Gans, S. Midollini, A. Vacca, *Adv. Inorg. Chem.* **2000**, *50*, 109 – 172.
[8] C. Y. Wong, J. D. Woolins, *Coord. Chem. Rev.* **1994**, *130*, 243 – 273.
[9] H. Schmidbaur, *Coord. Chem. Rev.* **2001**, *215*, 223 – 242.
[10] L. Richeldi, R. Sorrentino, C. Saltini, *Science* **1993**, *262*, 242 – 244.
[11] A. P. Fontenot, M. Torres, W. H. Marshall, L. S. Newman, L. S. , B. L. Kotzin, *Proc. Natl. Acad. Sci. USA* **2000**, *97*, 12717 – 12722.
[12] M. Amicosante, N. Sanarico, F. Berretta, J. Arroyo, G. Lombardi, R. Lecher, V. Colizzi, C. Saltini, *Hum. Immunol.* **2001**, *62*, 686 – 693.
[13] D. J. Price, J. G. Joshi, *J. Biol. Chem.* **1983**, *258*, 10873 – 10874.
[14] D. Asthagiri, L. R. Pratt, *Chem. Phys. Lett. B* **2003**, *371*, 613 – 619.
[15] F. Cecconi, C. A. Ghilardi, S. Midollini, A. Orlandini, *Inorg. Chem.* **1998**, *37*, 146 – 148.
[16] L. Scott, Z. Wang, B. L. Marrone, N. N. Sauer, *J. Inorg. Biochem.* **2003**, *94*, 5 – 13.
[17] Cambridge Structural Database, November (2005) Release, Cambridge Crystallographic Data Center, www.ccdc.cam.ac.uk.
[18] P. A. Frey, *J. Phys. Org. Chem.* **2004**, *17*, 511 – 520.
[19] J. S. Wright, D. J. Carpenter, D. J. McKay, K. U. Ingold, *J. Am. Chem. Soc.* **1997**, *119*, 4245 – 4252.
[20] D. Asthagiri, L. R. Pratt, H. S. Ashbaugh, *J. Chem. Phys.* **2003**, *119*, 2702 – 2708.
[21] M. J. Frisch, et al. Gaussian 03, Revision B.05, **2003**, Gaussian, Inc., Pittsburgh PA.
[22] C. L. Perrin, J. B. Nielson, *Annu. Rev. Phys. Chem.* **1997**, *48*, 511 – 544.
[23] M. Fleck, E. Tillmanns, S. Haussuhl, *Z. Kristallogr. New Cryst. Struct.* **1997**, *215*, 105 – 106.
[24] A. K. Shrive, H. A. Tharia, P. Strong, U. Kishore, I. Burns, P. J. Rizkallah, K. B. M. , Reid, T. J. Greenhough, *J. Mol. Biol.* **2003**, *331*, 509 – 523.